Structural and Mechanistic Basis for the Activation of a Low-Molecular Weight Protein Tyrosine Phosphatase by Adenine[†,‡]

Shuishu Wang,[§] Cynthia V. Stauffacher,[||] and Robert L. Van Etten*[,§]

Departments of Chemistry and Biological Sciences, Purdue University, West Lafayette, Indiana 47907

Received June 30, 1999; Revised Manuscript Received November 8, 1999

ABSTRACT: Although the activation of low-molecular weight protein tyrosine phosphatases by certain purines and purine derivatives was first described three decades ago, the mechanism of this rate enhancement was unknown. As an example, adenine activates the yeast low-molecular weight protein tyrosine phosphatase LTP1 more than 30-fold. To examine the structural and mechanistic basis of this phenomenon, we have determined the crystal structure of yeast LTP1 complexed with adenine. In the crystal structure, an adenine molecule is found bound in the active site cavity, sandwiched between the side chains of two large hydrophobic residues at the active site. Hydrogen bonding to the side chains of other active site residues, as well as some water-mediated hydrogen bonds, also helps to fix the position of the bound adenine molecule. An ordered water was found in proximity to the bound phosphate ion present in the active site, held by hydrogen bonding to N3 of adenine and Oδ1 of Asp-132. On the basis of the crystal structure, we propose that this water molecule is the nucleophile that participates in the dephosphorylation of the phosphoenzyme intermediate. Solvent isotope effect studies show that there is no rate-determining transfer of a solvent-derived proton in the transition state for the dephosphorylation of the phosphoenzyme intermediate. Such an absence of general base catalysis of water attack is consistent with the stability of the leaving group, namely, the thiolate anion of Cys-13. Consequently, adenine activates the enzyme by binding and orienting a water nucleophile in proximity to the phosphoryl group of the phosphoenzyme intermediate, thus increasing the rate of the dephosphorylation step, a step that is normally the rate-limiting step of this enzymatic reaction.

Phosphotyrosyl protein phosphatases are structurally diverse enzymes that are increasingly recognized as having fundamental roles in cellular processes, including effects on metabolism, cell proliferation, and differentiation (*1*). Low-molecular weight protein tyrosine phosphatases (low-M_r PTPases)[1] comprise a nearly ubiquitous group of 18 kDa enzymes. Except for the active site signature motif CX_5R-(S/T) that forms a phosphate-binding loop (P-loop), the sequences of these low-M_r PTPases are not at all similar with those of high-molecular mass PTPases or dual specificity phosphatases. They also possess a distinctly different three-dimensional structure (*2*). The overall architecture consists of a central four-stranded parallel β-sheet flanked by α-helices (*3*−*5*). There are, however, some features of the active site structure of low-M_r PTPases that are very similar to those of the larger PTPases. Despite the fact that it lacks the glycine-rich character, the phosphate-binding loop (P-loop) of low-M_r PTPases has a structure that is effectively identical to that of high-M_r PTPases (*2*, *6*-*10*). Indeed, the structure of the P-loop is the most conserved element in all PTPases. We have also pointed out that the P-loop has a rigid structure maintained in part by complex hydrogen bonding interactions and that its geometry favors optimal binding of the phosphate trigonal bipyramidal transition state structure (*11*−*14*). Both high- and low-M_r PTPases have deep active site cavities, lined with aromatic and/or hydrophobic residues. The aspartic acid residue that functions as a proton donor for the leaving group is also in a similar position relative to the P-loop (*2*, *3*, *15*). In high-M_r PTPases, this aspartic acid residue is on a movable loop that closes upon substrate binding (*16*). NMR solution structure data strongly suggest that the loop containing an aspartic acid residue is similarly mobile in the low-M_r PTPases (*4*). Although a crystal structure of the ligand-free form is not yet available, crystal structures of low-M_r PTPases with various ligands show that the loop containing the proton donor aspartic acid and two aromatic residues that form one wall of the active

[†] This research was supported by American Cancer Society Grant NP-946 awarded to C.V.S. and by United States Department of Health and Human Services Research Grants GM 27003 to R.L.V.E. and CA 82673 to C.V.S. Crystallographic facilities were supported in part by a National Cancer Institute grant to the Purdue University Cancer Center.

[‡] The atomic coordinates of the LTP1-C13A mutant complexed with *p*NPP have been deposited with the Protein Data Bank under file name 1D2A.

* To whom the correspondence should be addressed. Fax: (765) 494-0239.

[§] Department of Chemistry.

[||] Department of Biological Sciences.

[1] Abbreviations: PTPase, protein tyrosine phosphatase; low-M_r PTPase, low-molecular weight protein tyrosine phosphatase; high-M_r PTPase, high-molecular weight protein tyrosine phosphatase; BPTP, bovine low-M_r protein tyrosine phosphatase; LTP1, low-M_r PTPase from *Saccharomyces cerevisiae*; P-loop, phosphate-binding loop; *p*NPP, *p*-nitrophenyl phosphate; Bis-TRIS, bis(2-hydroxyethyl)iminotris(hydroxymethyl)methane; rmsd, root-mean-square deviation; PEG, polyethylene glycol.

10.1021/bi991515+ CCC: $19.00
Published on Web 01/19/2000

Scheme 1

$$E + pNPP \underset{k_{-1}}{\overset{k_1}{\rightleftharpoons}} E \cdot pNPP \underset{k_{-2}}{\overset{k_2}{\rightleftharpoons}} E - P \underset{k_{-3}}{\overset{k_3}{\rightleftharpoons}} E \cdot P_i \underset{k_{-4}}{\overset{k_4}{\rightleftharpoons}} E + P_i$$

$$- pNP \qquad + H_2O$$

site cavity does exhibit large relative movements (*14*). These data suggest that this loop has a role similar to that in high-M_r PTPases with respect to substrate binding and recognition.

The similarity in active site structures between the low- and high-M_r PTPases is also a reflection of the fact that they share identical catalytic mechanisms (Scheme 1). The first cysteine residue of the active site signature motif of the low-M_r PTPases functions as a nucleophile (*17*). In the course of the enzymatic reaction, phosphotyrosine in the substrate binds in the active site with its three anionic oxygen atoms hydrogen-bonded to P-loop residues, which fixes the phosphorus atom in proximity to the nucleophilic side chain of cysteine (*3*, *14*, *16*, *18*). The Sγ atom of cysteine attacks the phosphate group as the proton donor aspartic acid donates a proton to the leaving group oxygen, resulting in the formation of a covalent phosphocysteine intermediate (*17*, *19*). The P-loop favors deep binding of the phosphate group, thereby lowering the activation energy and facilitating the formation of the phosphoenzyme intermediate (*14*). The second step of the overall hydrolysis reaction is carried out by attack of a water molecule on the phosphoenzyme intermediate to form inorganic phosphate (k_3 in Scheme 1). For the low-M_r PTPases, it has been well established that the dephosphorylation of the covalent phosphoenzyme is significantly slower than the first step ($k_2 > k_3$), and is therefore the rate-limiting step of the enzymatic reaction (*20*, *21*).

The activity of low-M_r PTPases can be modulated by certain purines or purine derivatives. The activation of mammalian and avian low-M_r phosphatases by specific purine nitrogen bases, nucleosides, and nucleotides was first described several decades ago (*22*−*24*). The activity modulation of isoenzymes of human low-M_r PTPases by adenine and hypoxanthine has been carefully characterized (*25*). Despite the close structural similarity of adenine and hypoxanthine, it was found that the isoenzymes have different responses to the activity modulation. The **s** isoenzyme (or slow isoenzyme, so named from its electrophoretic mobility, and also called human B isoenzyme; *26*) is activated by adenine, and not affected by hypoxanthine, while the **f** isoenzyme (fast isoenzyme, also called human A isoenzyme) is inhibited in the presence of adenine, and activated by hypoxanthine. The rate enhancement by the activators has been found to be approximately 5-fold. Another study on the homologous bovine enzyme, BPTP, showed that the rate of hydrolysis of *p*-nitrophenyl phosphate (*p*NPP) is also activated by adenine and exhibits a similar rate enhancement (*27*).

The mechanism of the activation of the low-M_r PTPases by purines was not previously understood. In a prescient study, Tanizaki et al. (*23*) suggested the existence of a specific site on the enzyme that was capable of binding the purine effectors. Importantly, they demonstrated that the mechanism of activation did not involve transphosphorylation to the purine. Dissing et al. (*25*) suggested that the effectors must bind at a site different from the substrate-binding site. However, from the structures of the low-M_r PTPases, it was not apparent that such an effector binding site existed. Moreover, the chemical basis of the activation phenomenon was completely unknown.

Studies of the yeast enzyme appeared to offer the possibility of solving this puzzle. The low-M_r PTPase from the yeast *Saccharomyces cerevisiae*, LTP1, shows substrate specificity toward artificial substrates that is generally similar to that exhibited by the homologous mammalian enzymes, although it possesses a somewhat lower catalytic activity (*27*). However, it is even more effectively activated by adenine, bringing its activity to a level comparable with that of its vertebrate counterparts. For example, when using *p*NPP as a substrate, LTP1 can be activated in the presence of 5 mM adenine by more than 30-fold at 37 °C. Although the extent of activation of LTP1 by purines is larger than that observed with the human and bovine enzymes, other features of the interaction of purine and protein appear to be very similar. Binding of an adenine molecule quenches the fluorescence of a tryptophan that is found near the active site cleft of the low-M_r PTPases (*28*). Using fluorescence quenching techniques, the dissociation constants of the enzyme−adenine complexes have been determined to be about 3 mM for both the yeast LTP1 and bovine BPTP enzymes. LTP1 has a structural fold that is effectively identical to that of the mammalian low-M_r PTPases (*14*). Consequently, structural studies of the yeast enzyme in the presence of purine activators offered the promise of providing a general explanation for this activation phenomenon.

In this paper, we present a structure of yeast low-M_r PTPase, LTP1, complexed with adenine at 1.9 Å resolution. The crystal structure shows clearly how the adenine molecule binds in the active site cavity, while solvent kinetic isotope effects provide additional insights into the activation mechanism. These points are considered together with a brief discussion of the differences in activity modulation by the different effectors and related enzymes.

EXPERIMENTAL PROCEDURES

Protein Preparation. The cloning, expression, and purification of wild-type LTP1 were as described in Ostanin et al. (*27*). The purified enzyme was passed through a Sephadex G-25 desalting column to remove phosphate ion from the sample for kinetic and activity measurements. An inactive C13A mutant of LTP1, in which the nucleophilic cysteine was replaced with alanine, was prepared by site-directed mutagenesis as previously described (*14*).

Protein Crystallization. Solutions of the purified mutant C13A were exchanged into 5 mM NaOAc (pH 5.0) plus 10 mM NaCl, and were concentrated to approximately 10 mg/mL for crystallization experiments. The sitting drop vapor diffusion method was used. In each drop, 5 or 10 μL of protein solution was mixed with the same volume of well buffer. Crystals were obtained in approximately 1 week from drops set up with a well buffer of 12−18% PEG 3400, 50 mM NaCl in 100 mM Bis-TRIS buffer (pH 7.0), 20 mM

Table 1: Data Processing and Refinement Statistics

space group	$P2_12_12_1$
unit cell parameters (Å)	$a = 51.5$, $b = 63.3$, $c = 97.6$
resolution range (Å)	40−1.9
no. of unique reflections (no. of total observations)	22621 (327192)
completeness (%) (last bin completeness)	87.6 (39.3)
R_{sym}[a]	0.063
resolution range for refinement (Å)	12−1.9
total number of protein atoms	2548
average *B* factors of protein atoms (Å^2)	19
total number of other molecules	300 (water), 2 (PO_4), 1 (adenine), 1 (chloride)
average *B* factors of other molecules (Å^2)	27 (water), 19, 16 (PO_4), 18 (adenine), 14 (chloride)
rmsd for bond lengths (Å)	0.010
rmsd for bond angles (deg)	1.42
R_{free}[b]	24.4
R_{work}[b]	18.1

[a] $R_{sym} = \Sigma|(I_{hkl} - \langle I_{hkl}\rangle)|/\Sigma I_{hkl}$, where $\langle I_{hkl}\rangle$ is the average of I_{hkl} over all symmetry equivalents. [b] $R = \Sigma(|F_{obs} - k|F_{calc}||)/\Sigma|F_{obs}|$, where $|F_{obs}|$ and $|F_{calc}|$ are the absolute values of the observed and calculated structure factors, respectively, and k is the scale factor between the summation of the absolute values of the observed structure factors and that of the calculated structure factors. *R* factors were calculated using data in the resolution range shown for refinement without a σ cutoff. R_{free} (*49*) was calculated with a set of randomly selected data (8%) not used in the refinement. R_{work} was calculated against the data used in the refinement.

sodium phosphate, and 20 mM adenine at 20 °C. The dimensions of the biggest crystals were approximately 0.2 mm × 0.5 mm × 1 mm.

Data Collection. X-ray diffraction data were collected on an R-axis II imaging plate system (Molecular Structure Corp.) mounted on a Rigaku RU200 rotating anode X-ray generator operating at 50 kV, 100 mA. The data were collected from a single crystal under cryogenic conditions at approximately −150 °C. The cryogenic solvent contained 14% PEG 3400, 100 mM Bis-TRIS (pH 7.0), 50 mM NaCl, and 20 mM adenine with 16% glycerol added. The crystal was first soaked in the cryosolution with 1% glycerol, and the concentration of glycerol was gradually increased to 16%. The crystal was flash-frozen in a cryostream of N_2, and diffracted to better than 1.9 Å resolution. The data were indexed and integrated using the program DENZO (*29*), and scaled with the program SCALEPACK (*29*). The R_{sym} for the entire data set is 6.3%. The completeness of the data at resolutions higher than 2 Å is very low, because these diffraction spots were collected on the corners of the image plates. The crystal is in space group $P2_12_12_1$ with unit cell dimensions $a = 51.5$ Å, $b = 63.3$ Å, and $c = 97.6$ Å. There are two molecules (designated as molecules A and B) in one asymmetric unit with a Matthews volume of 2.14 Å^3/Da (*30*). The data processing statistics are summarized in Table 1.

Structure Determination. The molecular replacement method (*31*) was used to obtain the initial phase information for the observed individual reflections, using the crystal structure of wild-type LTP1 as a search model (*14*). A clear solution with positions for two molecules was found with a correlation coefficient of 0.748, and an *R* factor of 38.3% after running the program AMoRe (*32*). Electron density maps calculated from this initial model showed clear density for the adenine molecule in the active site of one of the two molecules in the asymmetric unit (designated as molecule B). The other molecule (molecule A) did not have defined density for adenine, nor was density for adenine found anywhere else in the crystal structure. Density that was well fitted by a phosphate ion was present in the active sites of both molecules A and B. The program O (*33*) was used for displaying electron density and manual model fitting. The model was refined using the program XPLOR (*34*), with noncrystallographic symmetry restraints. The final R_{work} is 18.1%, and R_{free} is 24.4% (Table 1). The final model contains 156 residues (from residue 5 to 160) for both molecules A and B, 300 ordered water molecules, one adenine molecule, two phosphate ions, and one chloride ion. The chloride ion (*B* factor = 14 Å^2) was found in the crystal structure near the active site of molecule A. It is almost coplanar with the Oγ1 atom of Thr-48, the Nδ2 atom of Asn-100, and the Nδ2 atom of Asn-97 with a distance of 2.92, 3.16, and 3.20 Å, respectively. When it was modeled as a water molecule, a very strong peak of difference electron density persisted, and the putative water molecule would have had a *B* factor below 2.0.

Protein Activity Assays, Kinetic Measurements, and Solvent Isotope Effect Studies. Protein activity was assayed at 37 °C in 100 mM NaOAc buffer (pH 5.0), with 1 mM EDTA and an ionic strength of 150 mM adjusted by adding NaCl. The kinetic parameters of wild-type LTP1 were measured using *p*NPP as a substrate in the presence and absence of 5 mM adenine, in both H_2O and D_2O, at pH values from 4.5 to 8.0. For each V_{max} and K_m determination, at least nine different substrate concentrations were used. The reaction rate was determined by monitoring the release of inorganic phosphate using a Malachite Green assay procedure (*35*) or by monitoring the release of *p*-nitrophenolate by measuring the absorbance at 405 nm as described by Davis et al. (*36*). The values were fitted to the Michaelis−Menten equation using the computer program Psiplot (Poly Software International, Sandy, UT).

RESULTS

Overall Structure and Crystal Packing. The refinement statistics are shown in Table 1. The LTP1 model contains 156 amino acid residues in both molecules A and B. No electron density was seen for the first four N-terminal residues of either molecule, presumably due to the high flexibility of these residues. There are two phosphate ions in the structure, one at the active site of each protein molecule. These phosphate ions exhibit strong hydrogen bonds to the phosphate-binding loop (P-loop). Initial electron density clearly indicated that an adenine molecule was in the active site of one of the molecules (molecule B) in the asymmetric unit. Final $2F_o - F_c$ electron density showed that the adenine molecule is very well ordered and is present with high occupancy (Figure 1).

The C13A−adenine complex crystal exhibits crystal packing different from that of both the wild-type crystal and the C13A−*p*NPP complex crystal, although they are also in space group $P2_12_12_1$ (*14*). However, there is a similar noncrystallographic dimer with the active sites of the two molecules facing each other. The rmsd between the Cα atoms of the C13A−adenine dimer and the C13A−*p*NPP dimer is about 0.6 Å. There is noncrystallographic 2-fold symmetry between the two molecules in the dimer, with the symmetry

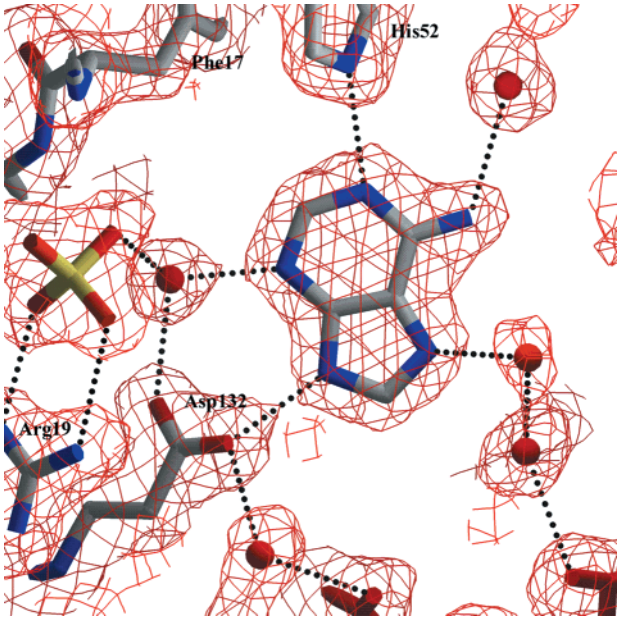

FIGURE 1: Electron density map ($2F_o - F_c$) showing the adenine molecule bound at the active site of molecule B in the LTP1−adenine complex structure. The electron density was calculated with phases from the final model refined at 1.9 Å, and contoured at the 1.0σ level. The figures were generated with the program Setor (*50*). Also shown is a phosphate ion, tightly bound in the active site by the backbone NHs of the P-loop. An ordered water molecule, w141, is held between the phosphate ion and adenine by hydrogen bonds to the phosphate ion, adenine, and Asp-132.

axis close to the active site on the surface where the two molecules pack. The interactions between the two molecules on this packing interface are closely similar to those of wild-type LTP1 (*14*). There are aromatic interactions between the two Tyr-51 rings at the entrance to the active site, two symmetric hydrogen bonds between the carbonyl oxygen of Asp-132 in one molecule and the Nϵ1 atom of Asn-99 in the other molecule, and hydrophobic interactions between the two Leu-14 side chains. An extensive water-mediated hydrogen-bonding network also appears to play an important role in the tight binding interaction between the two molecules. Most of these water molecules are highly ordered, with *B* factors similar to those of average protein atoms.

Adenine Binding Interactions. The adenine molecule is very well ordered, with an average *B* factor of 18 Å^2. It is found in the active site located above the bound phosphate ion (Figure 2). The adenine amino group faces out, toward the entrance of the active site cleft, while its N3 atom faces the bottom of the active site cavity toward the bound phosphate ion. The adenine molecule does not have any direct interactions with the backbone atoms of protein. Rather, it is sandwiched between the side chains of Tyr-51 and Trp-134, and further surrounded by the side chains of Asp-132, Tyr-135, Phe-17, His-52, and Leu-14. The side chain of Trp-134 stacks flat against the adenine ring, while the Tyr-51 ring tilts about 30° and shifts toward the amino group of adenine. His-52 and Phe-17 are present at one end of the adenine molecule, with the Nϵ atom of His-52 forming a hydrogen bond to N1 of adenine. The N9 atom of adenine forms a hydrogen bond to Asp-132. Two water molecules, w15 and w262, which hydrogen bond to each other and bridge the hydroxyl groups of Tyr-135 and Tyr-51, respectively, are above the five-member ring of adenine, with w262 hydrogen bonding to the N7 atom of adenine.

The N3 atom of adenine hydrogen bonds to a well-defined water molecule, w141 (Figure 1). This water molecule has a low *B* factor of 14 Å^2, which is very similar to the *B* factors of the nearby atoms of protein, phosphate ion, and adenine. It hydrogen bonds to O4 of the bound phosphate (distance of only 2.4 Å) and the Oδ1 atom of Asp-132 (2.82 Å). Its distance from the N3 atom of adenine is also short (2.55 Å). Although this water molecule is also moderately close

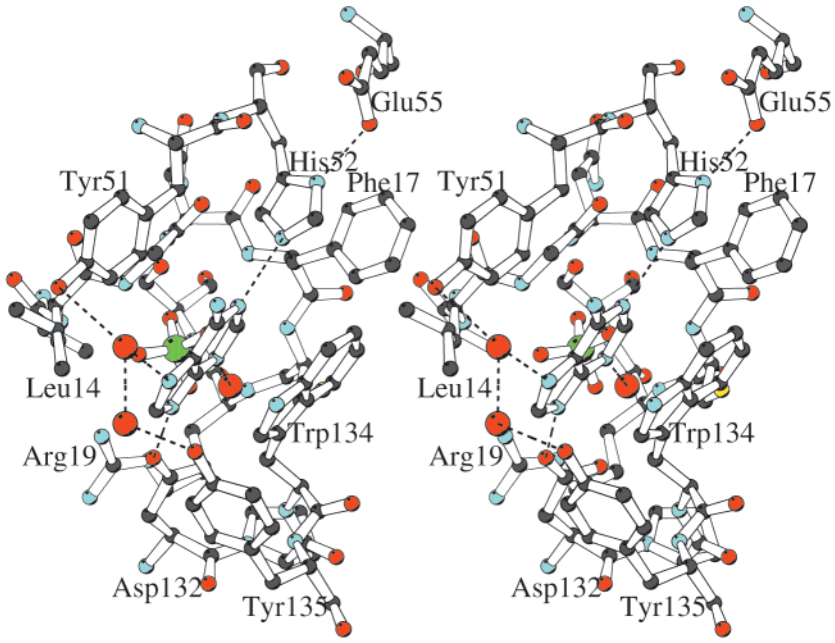

FIGURE 2: Stereoview of the adenine molecule bound in the active site of molecule B. The adenine is located above the inorganic phosphate molecule bound in the phosphate-binding loop. It is sandwiched between side chains of Trp-134 and Tyr-51, and also surrounded by the hydrophobic or aromatic side chains of Leu-14, His-52, Phe-17, and Tyr-135. The hydrogen bonds between the adenine and protein atoms or water molecules are shown, as well as those among Tyr-51, Tyr-135, and two water molecules. The side chain of Glu-55 is near the side chain of His-52, with a hydrogen bond between them. The stereoplots were generated with the program Molscript (*51*).

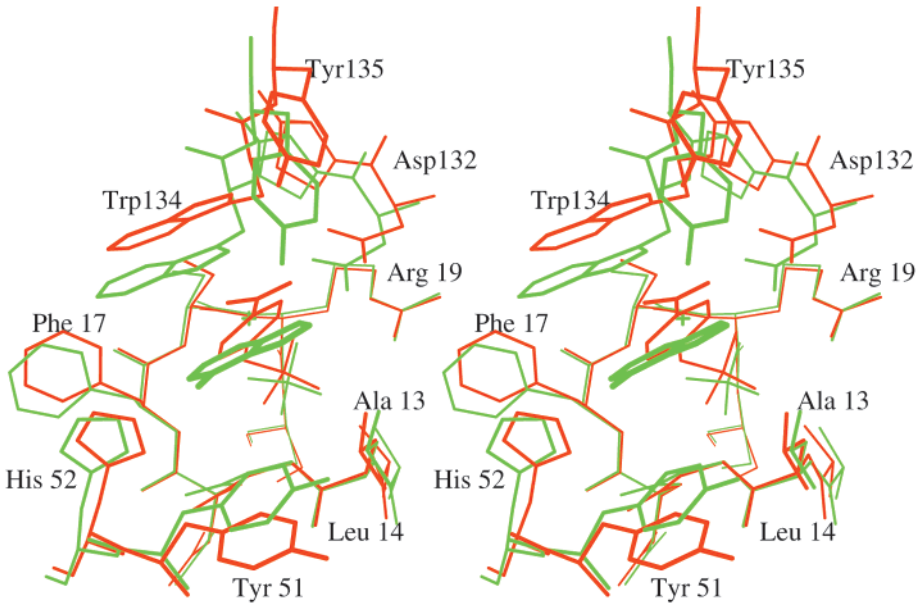

FIGURE 3: Stereoplot of the superposition between the active sites of the LTP1−adenine complex and of the LTP1−*p*NPP complex. The adenine complex is green, and the *p*NPP complex is red. The P-loop atoms of these two subunits align very well, but the residues lining the walls exhibit shifts in their positions. The adenine molecule binds in the active site at the same position as the *p*-nitrophenyl moiety of *p*NPP.

to the Sγ atom of Cys-18, there is not a favorable hydrogen bond because the distance is 3.18 Å and the Cβ−Sγ−w141 angle is only 84.3°. In protein molecule A, which does not contain adenine, there is also a bound water molecule, but it is shifted up 0.5 Å relative to the orientation seen in Figure 1, and is bound only to O4 of the phosphate.

A superposition between the C13A−adenine complex and the C13A−*p*NPP substrate complex (*14*) shows that adenine occupies a position where the leaving group (the *p*-nitrophenol moiety in the case of *p*NPP) of the substrate would be located (Figure 3). It is also obvious from the structure superposition that the binding of adenine is accommodated by shifting the flexible loop containing Asp-132, Trp-134, and Tyr-135, and also swinging the side chain of Tyr-51 toward the center of the active site cavity.

Comparison of the Two Molecules in the Asymmetric Unit. For the most part, the two protein molecules in the asymmetric unit, one with and one without adenine, are effectively identical, and exhibit similar *B* factors for the corresponding residues. However, a superposition of the two active sites clearly shows that the aromatic residues that are present on the walls of the active site cavity have undergone some significant shifts (Figure 4). The Tyr-51 side chain has a totally different conformation, with an rmsd between the two of more than 4 Å. This change in position reflects the structure of the unliganded enzyme, where Tyr-51 has not swung into position to sandwich an adenine molecule. These two forms in the asymmetric unit occur as an indirect consequence of the face-to-face crystal packing of the LTP1 molecules. If the side chain of Tyr-51 in molecule A (without adenine) had the same conformation as in molecule B, the two Tyr-51 side chains would directly clash with each other in the crystal. Thus, the binding of adenine in one molecule of the asymmetric unit dictates the positions of the side chain of Tyr-51 in the other protein molecule against which it can pack, selecting unliganded molecules as partners to give the observed noncrystallographic dimer. The loop that includes Trp-134 and Tyr-135 also exhibits a large shift in the

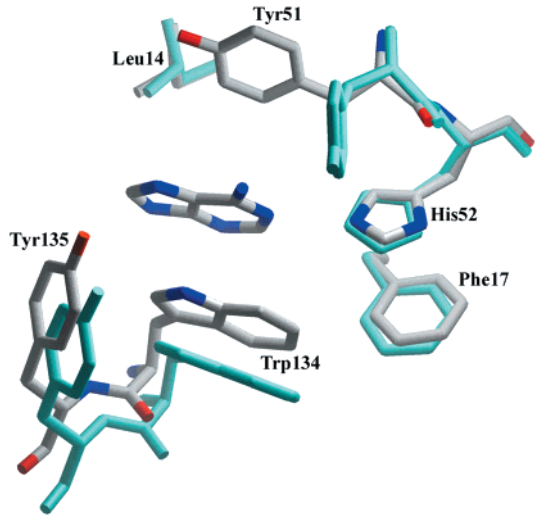

FIGURE 4: Superposition of the residues lining the walls of the active site cavities of molecules A and B. Molecule B with the bound adenine is colored by element, with light gray for the carbon atoms, while residues of molecule A are cyan. Both the main chain and side chain atoms on the loop containing Trp-134 and Tyr-135 exhibit a shift of more than 1 Å. The side chain of Tyr-51 has a different conformation in the two molecules.

superposition of the active sites. In the active site with the adenine molecule, this loop (both main chain and side chain atoms) moves toward the center of the active site cavity so that the side chain of Trp-134 is in an optimal position, together with the side chain of Tyr-51, to sandwich the adenine molecule. When the structure superposition is based on the Cα atoms of the P-loops (rmsd of 0.14 Å), both main chain and side chain atoms of the loop containing Asp-132, Trp-134, and Tyr-135 shift more than 1 Å (Figure 4).

Solvent Isotope Studies. As already noted, this crystal structure of the C13A−adenine complex reveals a water molecule tightly bound to N3 of adenine, O4 of phosphate ion, and Oδ1 of Asp-132. Such a water molecule would be well positioned to act as a reactant with the phosphoenzyme

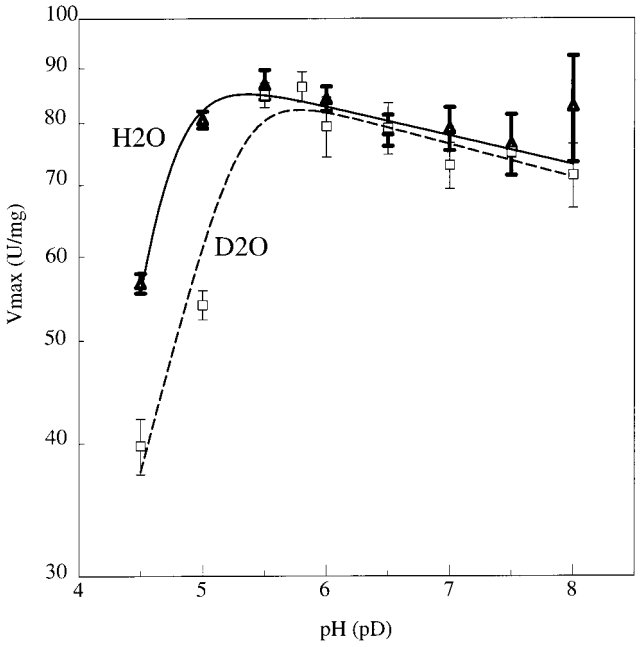

FIGURE 5: V_{max}−pH(pD) curves in the presence of 5 mM adenine in H_2O (△) and D_2O (□). Experimental conditions are as described in Experimental Procedures. The error bars represent the 95% confidence range calculated by the program PsiPlot.

intermediate in the rate-limiting dephosphorylation step of the enzymatic reaction. Two mechanisms could be envisioned. The N3 atom of adenine or the Oδ1 atom of the Asp-132 could possibly function as general base catalyst, extracting a proton from the water as a new bond is formed to phosphorus. Alternatively, the function of the adenine could be simply to bring an oriented water molecule into proximity to the phosphoenzyme intermediate.

As an experimental test of these alternatives, we measured the solvent deuterium isotope effect in the presence and absence of adenine. In the absence of adenine, there is no solvent isotope effect (data not shown). This is consistent with previous results obtained in studies on the bovine enzyme (*21*). In that case, although there is one proton "in flight" in the transition state for the phosphorylation process, there is no solvent isotope effect on k_{cat}, which is the rate-limiting dephosphorylation step of the phosphoenzyme intermediate. Figure 5 shows the results of the solvent isotope studies on LTP1 in the presence of 5 mM adenine. At low pH, LTP1 has higher activity in H_2O than in D_2O. However, at pH $\geq$5.5, the enzyme has effectively identical activities in H_2O and D_2O. This clearly indicates that there is no solvent isotope effect in the enzymatic dephosphorylation reaction. The apparent kinetic isotope effect at low pH is readily interpreted as a pK_a shift of a weak acid group on the enzyme when the solvent is changed from H_2O to D_2O (*37*).

DISCUSSION

Adenine has been shown to be a very good activator for LTP1 (*27*). The structural results presented here show that a well-defined adenine molecule is bound in the active site together with an ordered water molecule, at a position where the leaving group of the substrate would have been (Figure 3). The identification of such an adenine binding site is consistent with earlier findings by Tanizaki et al. (*23*), who concluded that purine activators of low-M_r acid phosphatase from bovine brain bind at a site where glycerol attacks the phosphoryl enzyme, and that such activators also inhibit the transphosphorylation to glycerol. The nature of the adenine binding site is not entirely consistent with the conclusions of Dissing et al. (*25*). In analyzing their data, they used a model which assumed that activators bind to both the free enzyme and the enzyme−substrate complex, and they concluded that the activators must bind at a site different from the active site. Nevertheless, they did point out the possibility that the effector might bind in the active site, replacing the leaving group on the reaction pathway.

In our structure, only one molecule (B) of the noncrystallographic dimer has an adenine molecule in the active site. The other molecule (A) has a different side chain conformation of Tyr-51 as a result of the crystal packing, and it does not show the sandwich of the adenine molecule with the side chain of Trp-134. A large shift of the loop containing Trp-134 and Tyr-135 was observed in molecule B relative to molecule A (Figure 4). This loop, which also contains the proton donor Asp-132 that functions as a general acid and donates a proton to the leaving group, has been found to be highly flexible (*14*). The corresponding loop in a high-M_r PTPase has been found to be in an open conformation and to close upon substrate binding (*15*, *16*, *18*). Such mobile peptide loops are also of considerable importance in other examples of enzymatic catalysis (*38*). In the case presented here, it is likely that in the free (unliganded) low-M_r PTPase, this loop is in an open conformation that effectively reduces the energetic favorability for adenine binding, thus explaining the fact that adenine is not effective as a competitive inhibitor.

The further finding of an ordered water molecule (w141) in the active site serves to explain how adenine activates the enzyme by increasing the rate of the dephosphorylation of the phosphoenzyme intermediate. It has been well established that all the PTPases catalyze the hydrolysis of phosphorylated substrates by going through a double-displacement mechanism. For the low-M_r PTPases, the phosphorylation of the enzyme to form a covalent phosphoenzyme intermediate is normally the rapid reaction step, while the dephosphorylation of the phosphoenzyme intermediate is the rate-limiting step of the overall reaction (i.e., $k_2 > k_3$ in Scheme 1). Thus, the rate constant of the phosphorylation step (k_2) for BPTP at pH 5.0 and 37 °C is 540 s^{-1} with *p*NPP as the substrate, and that of the dephosphorylation step (k_3) is 36.5 s^{-1} (*20*). Similarly, the rate constants of the phosphorylation (k_2) and dephosphorylation (k_3) steps for LTP1 have been determined to be 34 and 1.5 s^{-1}, respectively, at 25 °C and pH 6.0 with *p*NPP as the substrate (H. Kirsch, C. Pokalsky, and R. L. Van Etten, unpublished results).

To facilitate comparisons with the structure of LTP1 substrate complexes, an inactive C13A mutant was employed here. As a consequence of the mutation of Cys-13 to alanine, which has a smaller side chain and is neutral compared to the negatively charged cysteine side chain, the phosphate group is able to bind more deeply in the active site of the mutant (*14*). The position of the phosphorus atom in the phosphate group is similar to the position of the phosphorus atom of the phosphoenzyme intermediate. This can be clearly seen from the superposition of the active sites between the

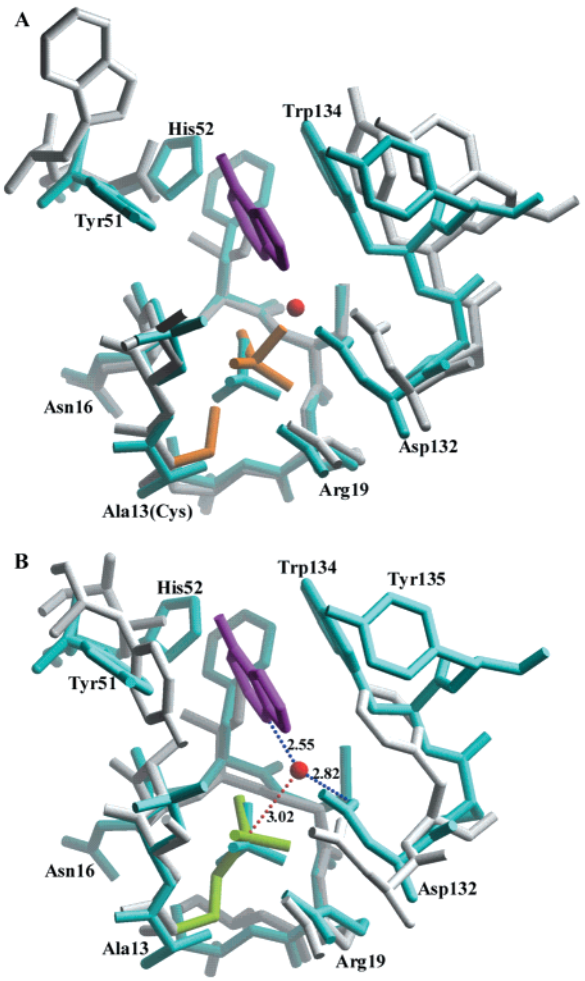

FIGURE 6: (A) Structural superposition between the active site residues of the LTP1−adenine complex and the BPTP−VO_4 complex (*12*). The superposition is based the positions of Cα atoms in the P-loop. LTP1 is cyan, with the adenine molecule magenta and the bound water (w141) red. The BPTP−VO_4 complex is light gray. The labels are for the residues in the LTP1 protein, where Cys-13 was mutated into an alanine. (B) Structural superposition between the active site residues of the LTP1−adenine complex and the PTP1B phosphoenzyme intermediate structure (*40*) based on the Cα atoms of the P-loop residues. The LTP1−adenine complex is cyan as in panel A. Residues from PTP1B are light gray except for the phosphocysteine group, which is green. The distance between the water molecule (w141) in the LTP1−adenine complex and the phosphorus atom of the phosphoenzyme intermediate in PTP1B is shown, together with the hydrogen bonds from w141 to adenine and to Asp-132.

C13A−adenine complex and the BPTP−vanadate complex (Figure 6A). Vanadate ion can inhibit phosphomonoesterases by forming a trigonal bipyramidal complex with the enzyme that resembles the transition state (*39*). In the case of low-M_r PTPases, the crystal structure of the vanadate complex shows that the vanadium atom is covalently linked to the nucleophilic cysteine at the active site (*12*). Thus, its position is closely similar to that of the phosphoryl group in the phosphoenzyme intermediate. A structure of the phosphoenzyme intermediate of a high-molecular weight PTPase, PTP1B, has been reported (*40*). Although the P-loop sequence of PTP1B (CSAGIGRS) is very different from that of the low-M_r PTPases (CLGNFCRS in LTP1), the structure of the backbone of the P-loop is very well conserved (*2*, *14*). Superposition of the active site residues between the LTP1−adenine and PTP1B phosphoenzyme intermediate structures (Figure 6B) shows not only that the P-loops superimpose very well (rmsd for Cα atoms of 0.54 Å) but also that the residues lining the walls of the active site cavity and the proton donor aspartic acid residues are in closely similar positions. It is clear from the structure superposition that the phosphate ion of the C13A−adenine structure is at the same position as the phosphoryl group of the PTP1B phosphoenzyme intermediate structure (*40*). Importantly, a water molecule in the C13A−adenine structure is hydrogen bonded to the N3 atom of adenine and to the Oδ1 atom Asp-132, thus fixing its position adjacent to the phosphoryl group. Consequently, this water is well positioned to function as a reactant in the dephosphorylation step of the enzymatic reaction.

Although the hydrolysis of this phosphoenzyme is specifically known to proceed with inversion of configuration around phosphorus (*41*), the nature of the possible catalytic enhancements required clarification. Because the water has hydrogen bonds to adenine and to the side chain of Asp-132, it could be possible for either the adenine molecule or the Asp-132 side chain to act as a general base to facilitate the attack of the water molecule on the phosphoenzyme intermediate. However, the solvent isotope effect studies show no solvent isotope effect for the reaction in the presence of adenine, just as earlier studies of the hydrolysis of *p*-nitrophenyl phosphate by the homologous bovine enzyme showed no such effect in the absence of purine activators (*21*). This clearly indicates that there is no *rate-determining* transfer of a solvent-derived proton in the transition state for the dephosphorylation of the phosphoenzyme intermediate. In other words, the adenine molecule activates the enzyme by holding an oriented water molecule in the proximity of the phosphorus atom of the phosphoenzyme intermediate. In this regard, it may be useful to note that given the necessary effective molarity and an activated leaving group, even a methyl ether may be an effective nucleophile (*42*).

Such a role for adenine in binding and orienting the nucleophilic water would be nicely in accord with the imaginative spatiotemporal hypothesis advanced by Menger (*43*, *44*). An in-line nucleophilic attack of a water molecule on the phosphoryl group requires the water molecule to be above the center of the three oxygen atoms of the phosphoryl group, with its oxygen atom exposed to the phosphorus atom. However, without any groups to fix its position, it is unfavorable for a water molecule to be centered above the phosphoryl group because of the repulsion from the negative charges on the oxygen atoms of the phosphoryl group. Hydrogen bonding to the N3 atom of adenine and the Oδ1 atom of Asp-132 not only fixes the position of the water molecule but also orients the water molecule so that its oxygen atom faces the phosphoryl group.

Adenine activates the mammalian low-M_r PTPases to a lesser extent than is observed for the yeast enzyme. The mammalian enzymes exhibit higher catalytic rates, so even in the absence of adenine, the rate of the respective dephosphorylation step is already faster. Another reason for the lower rate enhancement of mammalian low-M_r PTPases can be deduced from structural comparisons. In the crystal structure of the C13A−adenine complex, the adenine molecule is sandwiched by the side chains of Trp-134 and Tyr-51 (Figure 2). Hydrogen bonding to both His-52 and Asp-

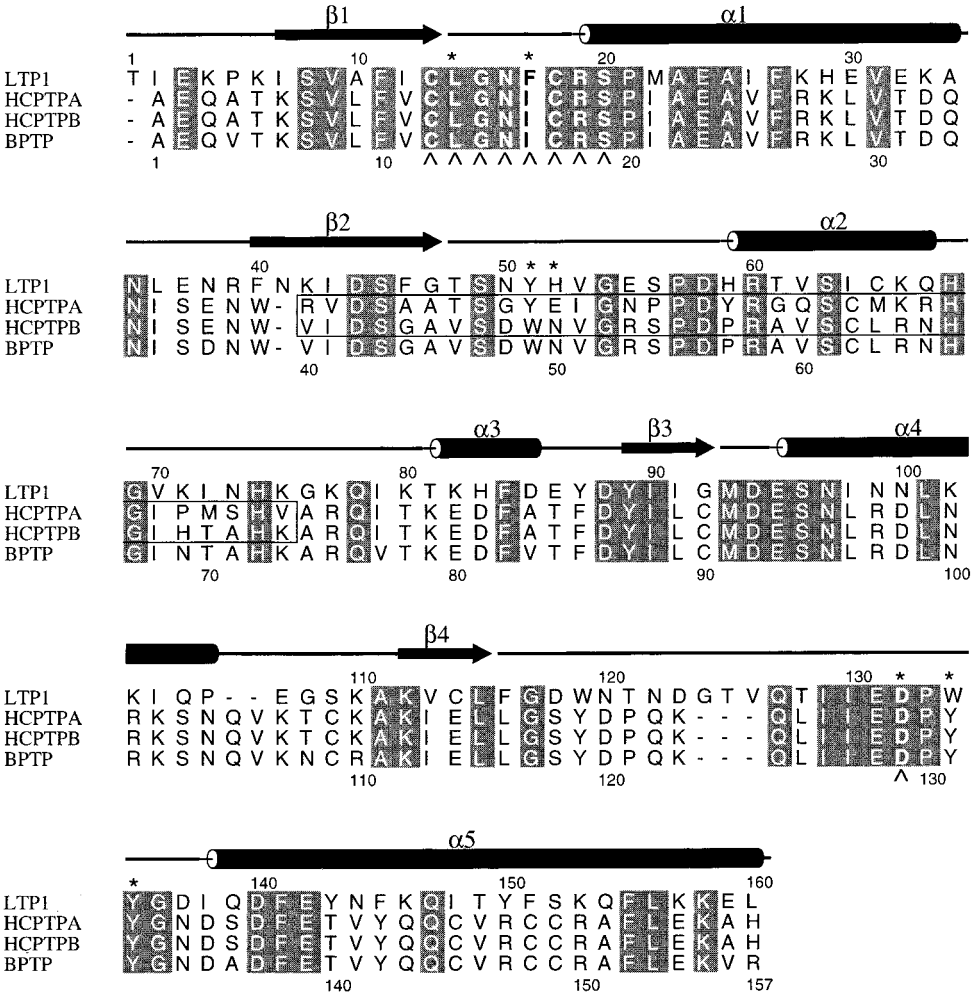

FIGURE 7: Sequence alignment of the low-molecular weight PTPases from yeast (LTP1), human (isoenzymes HCPTPA and HCPTPB; *26*), and bovine sources (BPTP). The sequences were aligned with the program Clustal-w, and the figure was generated with the program Alscript (*52*). Identical residues are highlighted in gray. The active site signature motif residues and the proton donor residue are labeled with a "∧" below the sequences. The residues interacting with adenine are indicated with a "*" on top. Boxed residues in the two human sequences constitute the variable loop that results from alternative mRNA splicing (*47*). Above the sequences are shown the secondary structure elements of LTP1.

132 side chains also appear to play an important role in fixing the position of the adenine molecule so that its N3 atom can be at the exact position to bind the nucleophilic water molecule (Figure 1). Although the aspartic acid, tryptophan, and tyrosine residues are conserved (albeit with the positions of tryptophan and tyrosine swapped), the His-52 of LTP1 is replaced by an asparagine in the bovine (BPTP) and human B (HCPTPB) enzymes (Figure 7). This substitution does not appear to change the affinity of the adenine appreciably. The dissociation constant of the enzyme−adenine complex was measured using the technique of tryptophan fluorescence quenching, and was found to be identical for both LTP1 and BPTP (*27*). However, the position of the adenine molecule would be somewhat shifted due to the changed hydrogen bonding pattern, and the catalytic efficiency as an activator would be affected.

Similar reasoning applies to the effect of hypoxanthine on the low-M_r PTPases. Hypoxanthine has been found to activate the **f** isoenzyme (HCPTPA) of human low-M_r PTPases, but has no effect on the activity of the **s** isoenzyme (HCPTPB) (*25*). We found that hypoxanthine also has very little effect on the activity of LTP1 (data not shown). In terms of activity modulation, LTP1 is thus similar to the human B isoenzyme (**s** isoenzyme), even though it has an overall sequence that is similar (39 and 40% identity for HCPTPA and HCPTPB, respectively) to those of both isoenzymes of human low-M_r PTPase (*27*). The difference between the structures of adenine and hypoxanthine exists only at the C6 position, where it is an amine on adenine and a carbonyl on hypoxanthine. However, this difference will result in a difference in the hydrogen bonding ability of the N1 atom. While the N1 atom of adenine is a good hydrogen bond acceptor, the N1 atom of hypoxanthine is protonated, and can only function as a hydrogen bond donor. In the structure of the LTP1−adenine complex, the N1 atom of adenine is hydrogen bonded to Nϵ2 of His-52. The position of His-52 is fixed by aromatic stacking with Phe-17, and a hydrogen bond is formed from its Nδ1 to the Oϵ1 atom of Glu-55 (Figure 2). Electrostatic interactions of a histidine residue with nearby negatively charged groups can greatly elevate the pK_a value of the histidine (*45*). Aromatic ring stacking of histidines with other aromatic side chains also contributes to pK_a elevations of histidine (*46*). Therefore, His-52 is likely to have an elevated pK_a and to be doubly protonated. As a result, it is not able to form a good hydrogen bond with hypoxanthine, thus causing the hypoxanthine molecule to

bind poorly or in a way which makes it unable to position the nucleophilic water molecule immediately adjacent to the phosphoryl group of the phosphoenzyme intermediate.

The only sequence differences between the two human isoenzymes (HCPTPA and HCPTPB) (Figure 7) are present in a segment from residue 40 to 73 in the mature human enzymes that are produced by alternative mRNA splicing (*26*, *47*, *48*). This segment is termed the variable loop (*3*, *13*, *26*). On the corresponding variable loop in the yeast enzyme, two residues were found to interact with the adenine molecule in the LTP1−adenine complex (Tyr-51 and His-52). These two residues are different in the human isoenzymes, with Tyr-49 and Glu-50 being present in HCPTPA as compared to Trp-49 and Asn-50 in HCPTPB. Therefore, in HCPTPA the two residues corresponding to those that sandwich the adenine molecule in LTP1 are both tyrosines, instead of one tyrosine and one tryptophan as in LTP1 and the human B isoenzyme. The Glu-50 in HCPTPA represents a somewhat larger and probably differently charged side chain compared to histidine or asparagine residues. Consequently, the effector molecules must bind in a different mode in the two human isoenzymes, resulting in different activity modulation by adenine and hypoxanthine.

In this work, we have deduced from the crystal structure of the LTP1−adenine complex the mechanism of activation of low-M_r PTPases by purines, a phenomenon that has been known for over three decades. We propose that an adenine molecule binds in the active site during the dephosphorylation step, which is the rate-limiting step of the normal enzymatic reaction, and brings a water molecule to the proximity of phosphoenzyme intermediate for more efficient nucleophilic attack.

ACKNOWLEDGMENT

We thank Dr. Etti Harms for preparing the LTP1-C13A mutant used in this study and for her helpful revisions of the manuscript.

REFERENCES

1. Lau, K. H., and Baylink, D. J. (1993) *Crit. Rev. Oncog. 4*, 451−471.
2. Zhang, M., Stauffacher, C. V., and Van Etten, R. L. (1995) *Adv. Protein Phosphatases 9*, 1−23.
3. Zhang, M., Van Etten, R. L., and Stauffacher, C. V. (1994) *Biochemistry 33*, 11097−11105.
4. Logan, T. M., Zhou, M.-M., Nettesheim, D. F., Meadows, R. P., Van Etten, R. L., and Fesik, S. W. (1994) *Biochemistry 33*, 11087−11096.
5. Su, X.-D., Taddei, N., Stefani, M., Ramponi, G., and Nordlund, P. (1994) *Nature 370*, 575−578.
6. Barford, D., Flint, A. J., and Tonks, N. K. (1994) *Science 263*, 1397−1404.
7. Hoffmann, K. M. V., Tonks, N. K., and Barford, D. (1997) *J. Biol. Chem. 272*, 27505−27508.
8. Fauman, E. B., Cogswell, J. P., Lovejoy, B., Rocque, W. J., Holems, W., Montana, V. G., Piwnica-Worms, H., Rink, M. J., and Saper, M. A. (1998) *Cell 93*, 617−625.
9. Nam, H.-J., Poy, F., Krueger, N. X., Saito, H., and Frederick, C. A. (1999) *Cell 97*, 449−457.
10. Yuvaniyama, J., Denu, J. M., Dixon, J. E., and Saper, M. A. (1996) *Science 272*, 1328−1331.
11. Evans, B., Tishmack, P. A., Pokalsky, C., Zhang, M., and Van Etten, R. L. (1996) *Biochemistry 35*, 13609−13617.
12. Zhang, M., Zhou, M., Van Etten, R. L., and Stauffacher, C. V. (1997) *Biochemistry 36*, 15−23.
13. Zhang, M., Stauffacher, C. V., Lin, D., and Van Etten, R. L. (1998) *J. Biol. Chem. 273*, 21714−21720.
14. Wang, S., Tabernero, L., Zhang, M., Harms, E., Van Etten, R. L., and Stauffacher, C. V. (2000) *Biochemistry* (in press).
15. Jia, Z. (1997) *Biochem. Cell Biol. 75*, 17−26.
16. Stuckey, J. A., Schubert, H. L., Fauman, E. B., Zhang, Z.-Y., Dixon, J. E., and Saper, M. A. (1994) *Nature 370*, 571−575.
17. Wo, Y.-Y. P., Zhou, M.-M., Stevis, P., Davis, J. P., Zhang, Z.-Y., and Van Etten, R. L. (1992) *Biochemistry 31*, 1712−1721.
18. Jia, Z., Barford, D., Flint, A. J., and Tonks, N. K. (1995) *Science 268*, 1754−1758.
19. Zhang, Z., Harms, E., and Van Etten, R. L. (1994) *J. Biol. Chem. 269*, 25947−25950.
20. Zhang, Z.-Y., and Van Etten, R. L. (1991) *J. Biol. Chem. 266*, 1561.
21. Zhang, Z.-Y., and Van Etten, R. L. (1991) *Biochemistry 30*, 8954−8959.
22. Di Pietro, D. L., and Zengerle, F. S. (1967) *J. Biol. Chem. 242*, 3391−3396.
23. Tanizaki, M. M., Bittencourt, H. M., and Chaimovich, H. (1977) *Biochim. Biophys. Acta 485*, 116−123.
24. Baxter, J. H., and Suelter, C. H. (1985) *Arch. Biochem. Biophys. 239*, 29−37.
25. Dissing, J., Rangaard, B., and Christensen, U. (1993) *Biochim. Biophys. Acta 1162*, 275−282.
26. Wo, Y.-Y. P., McCormack, A. L., Shabanowitz, J., Hunt, D. F., Davis, J. P., Mitchell, G. L., and Van Etten, R. L. (1992) *J. Biol. Chem. 267*, 10856−10865.
27. Ostanin, K., Pokalsky, C., Wang, S., and Van Etten, R. L. (1995) *J. Biol. Chem. 270*, 18491−18499.
28. Pokalsky, C., Wick, P., Harms, E., Lytle, F. E., and Van Etten, R. L. (1995) *J. Biol. Chem. 270*, 3809−3815.
29. Otwinowski, A. (1993) *DENZO, in Data Collection and Processing*, pp 56−62, Daresbury Laboratory, Warrington, U.K.
30. Matthews, B. W. (1968) *J. Mol. Biol. 33*, 491−497.
31. Rossmann, M. G., and Blow, D. M. (1962) *Acta Crystallogr. 15*, 24−31.
32. Navaza, J. (1994) *Acta Crystallogr. A50*, 157−163.
33. Jones, T. A., Zou, J. Y., Cowan, S. W., and Kjeldgaard, M. (1991) *Acta Crystallogr. A47*, 110−119.
34. Brunger, A. T., Kuriyan, J., and Karplus, M. (1990) *Acta Crystallogr. A46*, 585−593.
35. Baykov, A. A., Evtushenko, O. A., and Avaeva, S. N. (1988) *Anal. Biochem. 171*, 266−270.
36. Davis, J. P., Zhou, M.-M., and Van Etten, R. L. (1994) *J. Biol. Chem. 269*, 8734−8740.
37. Jencks, W. P. (1969) *Catalysis in Chemistry and Enzymology*, pp 250−253, McGraw-Hill Book Co., New York.
38. Wang, G. P., Cahill, S. M., Liu, X., Girvin, M. E., and Grubmeyer, C. (1999) *Biochemistry 38*, 284−295.
39. Van Etten, R. L., Waymack, P. P., and Rehkop, D. M. (1974) *J. Am. Chem. Soc. 96*, 6782−6785.
40. Pannifer, A. D. B., Flint, A. J., Tonks, N. K., and Barford, D. (1998) *J. Biol. Chem. 273*, 10454−10462.
41. Saini, M. S., Buchwald, S., Van Etten, R. L., and Knowles, J. (1981) *J. Biol. Chem. 256*, 10453−10455.
42. Winstein, S., Allred, E., Heck, R., and Glick, R. (1958) *Tetrahedron 3*, 1−13.
43. Menger, F. M. (1985) *Acc. Chem. Res. 18*, 128−134.
44. Menger, F. M. (1992) *Biochemistry 31*, 5368−5373.
45. Tishmack, P. A., Bashford, D., Harms, E., and Van Etten, R. L. (1997) *Biochemistry 36*, 11984−11994.
46. Loewenthal, R., Sancho, J., and Fersht, A. R. (1992) *J. Mol. Biol. 224*, 759−770.
47. Bryson, G. M., Massa, H., Trask, B. J., and Van Etten, R. L. (1995) *Genomics 30*, 133−140.
48. Dissing, J., and Johnsen, A. H. (1992) *Biochim. Biophys. Acta 1121*, 261−268.
49. Brunger, A. T. (1992) *Nature 355*, 472−474.
50. Evans, S. V. (1993) *J. Mol. Graphics 11*, 134−138.
51. Kraulis, P. J. (1991) *J. Appl. Crystallogr. 24*, 946−950.
52. Barton, G. J. (1993) *Protein Eng. 6*, 37−40.

BI991515+